SIN-CHN
SCIENTIFIC PRESS PTE.LTD.

Molecular & Cellular Biomechanics 2025, 22(1), 1022.
https://doi.org/10.62617/mcb1022

Article

A bio-mechanical study on ankle movements of basketball players combined with DFIS

Qiang Hou

Jiaozuo University, Jiaozuo 454000, China; yanyan_001705@163.com

CITATION

Hou Q. A bio-mechanical study on ankle movements of basketball players combined with DFIS. Molecular & Cellular Biomechanics. 2025; 22(1): 1022. https://doi.org/10.62617/mcb1022

ARTICLE INFO

Received: 5 December 2024
Accepted: 20 December 2024
Available online: 6 January 2025

Abstract: To reduce the frequency of ankle injuries in basketball players, many studies have been conducted on the biomechanics of ankle movements in basketball players. However, due to the unclear recognition of bone images, there are inaccuracies in bio-mechanical analysis. To address the aforementioned issues, this study combines a dual plane orthogonal fluorescence imaging system with magnetic resonance imaging technology to propose a new image modeling method. Comparing this method with other methods, the results show that this method has the highest data collection integrity, and the highest image clarity reaches 98.7%. The root mean square error of pixel differences in the image is the lowest, only 0.96%. By using this method to analyze the biomechanics of basketball players' lateral cutting movements, it is found that the strain and strain rate of the ankle anterior cruciate ligament decreases to 13.5% and 296%, respectively, when the athlete wears high top shoes. In addition, the basketball player's on-stage speed during lateral cutting movements is 2.23 m/s, which is higher than other states. Moreover, various reaction forces during lateral cutting movements first increase and then decrease with the movement cycle. The experimental results indicate that the proposed image modeling method can increase image clarity and improve the accuracy of bio-mechanical analysis. There is a certain correlation between the bio-mechanical changes of basketball players and the height of their shoe uppers.

Keywords: dual plane orthogonal fluorescence imaging system; magnetic resonance imaging technology; basketball players; ankle; biomechanics of action

1. Introduction

With the continuous improvement of living standards, people's attention to sports continues to deepen [1]. Basketball, as one of the most common sports, has gradually gained popularity among people [2]. In basketball, the ankle of a basketball player plays an extremely important role during exercise, as it can support and protect the joint, improving athletic performance [3]. Ankle sprain is a common sports injury among basketball players, which can lead to a decrease in their athletic ability, limited joint function, and ultimately affect their performance in games and training [4]. The biomechanics of ankle movement mainly studies the bio-mechanical characteristics of human movement and the mechanical laws of human movement movements, also known as sports biomechanics [5]. By analyzing the biomechanics of the ankle, basketball players can better master their sports skills and patterns, reduce the probability of ankle sprains, and thus better train and compete [6]. Many scholars have conducted research on ankle biomechanics. For example, Yu et al. [7] analyzed the biomechanics of movement and dynamic posture control between chronic ankle-joint and ankle-joint sprain individuals in order to study the empirical consensus of differences between the two groups. The results showed that the differences in biomechanics of movement between the two individuals could represent the empirical consensus of differences between individuals. In addition, Koldenhoven et al. [8] conducted a comparative experiment to analyze the main injury mechanisms of ankle sprains in chronic ankle patients and rehabilitation patients. The results showed that ankle eversion was the main injury mechanism of ankle sprains, and the accuracy of this result reached 89.7%. Wang et al. [9] analyzed the biomechanics of the ankle-joint of basketball players with chronic ankle instability during the three-step layup operation. The results showed that the maximum dorsiflexion angle of the ankle-joint increased and the peak time of ankle dorsiflexion torque was longer in basketball players with chronic ankle instability. Domínguez-Navarro et al. [10] investigated the effects of hip abductor and adductor strength on ankle biomechanics in female basketball players. They used Pearson correlation coefficient to analyze the impact of hip strength on balance and ankle range of motion. The results showed that the strength of hip abductor and adductor muscles had a certain impact on ankle biomechanics. However, in the above studies, when analyzing the biomechanics of ankle movement, the current research is not accurate enough due to the blurry medical images of ankle bone structure and poor completeness of ankle data collection. Therefore, proposing a method that can fully collect and clearly image ankle bone data is an urgent problem that needs to be solved.

The Dual Fluorescent Imaging System (DFIS) is an electronic measuring instrument used in the field of sports, which can collect and analyze three-dimensional motion data of human bones and joints [11]. It is applied to the collection of bio-mechanical data of basketball players' ankles, in order to improve the complete collection of ankle bone data during basketball players' exercise. This system is widely used in various fields due to its high data collection accuracy. For example, Wu et al. [12] compared the width of glenoid trajectories under dynamic and static conditions and proposed a method for collecting arm bone joint data based on the DFIS. The method was tested in practical situations, and the results showed that the completeness of effective data collection reached 92.3%. After collecting DFIS data, it is necessary to conduct bio-mechanical analysis of the movement, and register the ankle related data extracted from the DFIS with the skeletal structure image of the athlete's ankle during exercise, in order to obtain complete information about the athlete's ankle-joint movement during exercise. Magnetic Resonance Imaging (MRI) technology can generate high-resolution images, displaying the structure and function of bones and joints in detail, and is often used in various medical imaging [13]. For example, Arnold et al. designed a scanner based on MRI technology to improve the image clarity of outpatient neuroimaging. The scanner was compared with other scanners and the results showed that it could improve image clarity by 32.8% [14]. Applying this technology to the bio-mechanical analysis of basketball players' ankles, MRI technology can obtain ankle-joint images of athletes during exercise, and register the images with the data collected in the DFIS to model the ankle-joint movement of basketball players during exercise and analyze their biomechanics.

Overall, it can be concluded that there is still a problem of inaccurate analysis caused by occasional image blurring in current bio-mechanical analysis. To address the aforementioned issues, this study combines the DFIS with MRI technology and designs a bio-mechanical analysis method for DFIS-MRI. This study analyzes the biomechanics of ankle movement of basketball players at different shoe upper heights, in order to provide reasonable suggestions for basketball players and reduce the probability of ankle injuries. The innovation of the research lies in collecting ankle data of basketball players through the DFIS, and then using MRI technology to extract images of ankle bone structure. The collected data and extracted images are registered, and then 3D modeling is carried out to analyze the biomechanics of basketball players' ankle movement.

2. Methods and materials

2.1. Collection of sports biomechanics data based on DFIS

With the development of society and the increasing emphasis on physical health, the field of sports is receiving more and more attention from people. Basketball, as a common sport, has also gained increasing popularity among people, and at the same time, basketball teaching has also received widespread attention [15]. Sports biomechanics, also known as action biomechanics, is a mechanical study that investigates the mechanical characteristics and laws of human movement. By analyzing sports biomechanics, coaches and athletes can better understand and master the principles and laws of sports, thereby improving their sports skills and competitive level. At present, due to the technical deficiencies in the collection of athlete data in traditional sports biomechanics analysis, which leads to inaccurate and missing data collection, it is necessary to optimize the data collection technology. The DFIS is an electronic measuring instrument used in the field of sports science, which can collect and analyze three-dimensional kinematic data of human bones and joints. The data accuracy can reach sub-millimeter level, which can meet the standards in the field of motion analysis [16]. This study aims to improve the accurate analysis of the biomechanics of ankle movement in basketball players by using the DFIS to capture ankle movements during various exercises. The structure of the DFIS is shown in **Figure 1**.

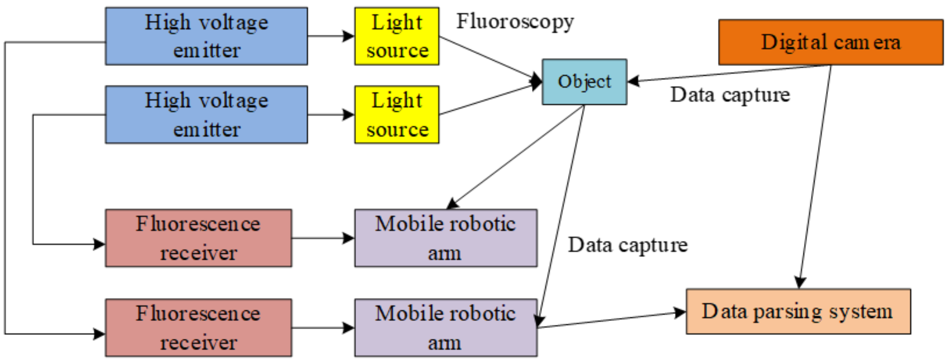

Figure 1. The DFIS structure.

As shown in **Figure 1**, the DFIS includes a light source setup for fluorescence fluoroscopy. Secondly, it also includes a device that matches the light source settings for receiving fluorescence and enhancing image information, to capture data on bone movement and ensure data reliability. In addition, the DFIS also includes digital cameras that affect data collection, as well as a data parsing system that processes and analyzes collected data to provide operational analysis results. Through the above structure, the DFIS can capture the degree of freedom movement of various joints during human motion, in order to provide more accurate bio-mechanical raw data of human motion. When analyzing sports biomechanics, it mainly includes the analysis of the operating state and laws of the studied object, generally including the object's velocity, acceleration, and displacement. The calculation is shown in Equation (1).

$$\begin{cases} v = s/t \\ a = (v_2 - v_1)/t \\ s = vt + 1/2(at^2) \end{cases} \tag{1}$$

In Equation (1), s represents displacement, v represents average velocity, t represents time, a represents acceleration, v_2 represents final velocity, and v_1 represents initial velocity. The study of the causes and laws of object motion in biomechanics requires the use of dynamic calculation, as shown in Equation (2).

$$\begin{cases} F = ma \\ p = mv \\ F_t = mv_t - mv_0 \end{cases} \tag{2}$$

In Equation (2), m represents mass, p represents momentum, F_t represents the impulse of the combined external force, and v_t represents the velocity at time t. Various bio-mechanical data of objects are accurately collected through the DFIS and then preprocessed.

2.2. MRI-based image extraction technology

However, to delve into the biomechanics of ankle movement in basketball players, ankle-related data first need to be gathered from the DFIS. Furthermore, it's crucial to align this data with images of the athlete's ankle skeletal structure during exercise to gain a comprehensive understanding of their ankle-joint movement. MRI is a medical imaging technique based on the phenomenon of nuclear magnetic resonance, which images the internal structure of the human body through the action of magnetic fields and radio frequency pulses [17]. The basic principle of this technology is shown in **Figure 2**.

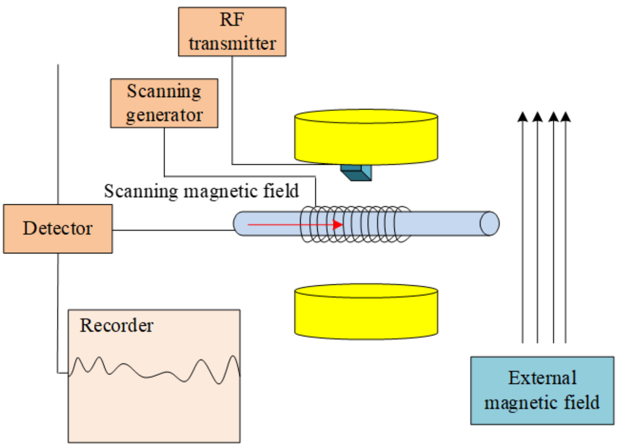

Figure 2. Principle of MRI technology.

As shown in **Figure 2**, MRI technology mainly consists of three steps: magnetic field preparation, pulse emission, and signal acquisition. This technology first requires placing the research object in a strong external magnetic field, which is typically generated by superconducting coils. This magnetic field will adjust the magnetic moment of the atomic nuclei inside the research object to be parallel to the main magnetic field. When the atomic nucleus is placed in the main magnetic field, the magnetic moment begins to rotate due to the distribution of magnetic field lines in the field. Then, by emitting pulses of a specific frequency, resonance electromagnetic waves are generated in the atomic nucleus, instantly flipping the magnetic moment of the atomic nucleus. Finally, when the RF pulse ends, the atomic nucleus will attempt to return to its initial state. During this process, the atomic nucleus will release energy in the form of electromagnetic radiation, which will be captured by the receiver in the MRI and converted into electrical signals, which will then be further converted into images. By aligning the images captured using MRI technology with the data acquired from DFIS, the precise position of the ankle-joint at every moment of movement can be determined, yielding information on the ankle-joint's range of motion. The core calculation of MRI technology is the calculation of magnetic resonance frequency, which is shown in Equation (3).

$$w = \gamma B_0 \tag{3}$$

In Equation (3), w represents the frequency of nuclear magnetic resonance, γ is the magnetic rotation ratio, and B_0 represents the strength of the external magnetic field. The calculation for the nuclear magnetic moment is shown in Equation (4).

$$\mu = \gamma P \tag{4}$$

In Equation (4), P represents angular momentum and μ represents nuclear magnetic moment. The calculation for the interval pixels between periodic motion artifacts of atomic nuclei is shown in Equation (5).

$$D = (TR * N * NEX)/T \tag{5}$$

In Equation (5), TR represents the repetition time, N represents the number of phase codes, NEX represents the number of repetitions, and T represents the motion period of the target artifact. After nuclear magnetic resonance, the signal acquisition is shown in Equation (6).

$$I(x,y) = \iint \rho(x,y)\exp[-I\gamma Bz(x,y)\alpha]dxdy \tag{6}$$

In Equation (6), $I(x,y)$ represents the strength of the received signal at spatial position (x,y), $\rho(x,y)$ represents the magnetization strength at the received signal position, $Bz(x,y)$ is the magnetic field strength at that position, and α is the pulse time. Through the above calculation, real-time motion images of the ankle of basketball players during exercise can be obtained. By combining these real-time motion images with the data analysis results obtained from the DFIS, a three-dimensional model of ankle-joint real-time motion can be constructed to analyze its bio-mechanical properties.

2.3. Analysis of ankle biomechanics of basketball players combining DFIS and MRI

In order to accurately analyze the biomechanics of basketball players' ankles, reduce ankle injuries, and improve their athletic performance, this study combines the DFIS with MRI technology to collect various motion data of basketball players during operation. Then, MRI technology is used to obtain ankle-joint images of basketball players during exercise. By registering the data obtained from the DFIS with the images obtained from MRI technology, the ankle-joint motion of basketball players during exercise is modeled to analyze their biomechanics. The data collection process of the DFIS for the ankle-joint of basketball players during exercise is shown in **Figure 3**.

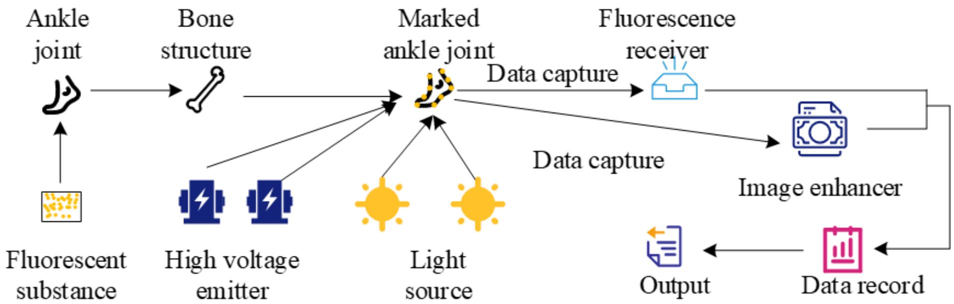

Figure 3. DFIS collection flow chart.

From **Figure 3**, the DFIS first uses special fluorescent substances to mark the skeletal structure of basketball players' ankle-joints, and then uses high-voltage emitters and light sources in the system to provide fluorescent perspective light. The system then captures bone structure data using a fluorescence receiver and image intensifier based on fluorescent labeling, and records changes in the position of the bone structure. The light sources in the DFIS present a mutually perpendicular relationship, which can scan the bone structure from different directions, ensuring the integrity and accuracy of the data. To solve the problem of image distortion, it is necessary to conduct calibration experiments in advance. A disk corrector is placed in the fluorescence receiving and image information enhancement device of the DFIS, which contains a rectangular array of steel balls. Based on the images received on the disk corrector and their relationship with the physical arrangement, Matlab software is used to obtain image calibration parameters. With these calibration parameters, the accuracy of the fluorescence imaging images is evaluated and batch calibration is carried out. The basic process of extracting ankle-joint images from basketball players using MRI technology is shown in **Figure 4**.

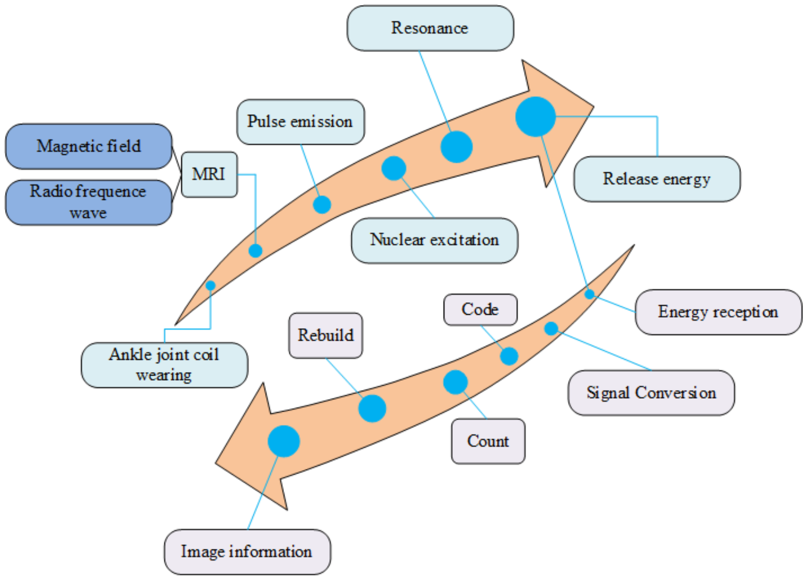

Figure 4. Flow chart of MRI image collection technology.

As shown in **Figure 4**, MRI technology first applies ankle-joint coils to basketball players to track and record changes in the ankle-joint. Then the MRI machine will generate a powerful magnetic field and radio frequency waves, which can penetrate the human body. The magnetic field is generated by the magnetic system of the MRI equipment, that is, the coil worn. Then, the radio frequency system of the MRI equipment emits pulses of specific frequencies, which excite the atomic nuclei in the ankle-joint, causing them to emit resonance and absorb energy. After the process is completed, the atomic nuclei in the ankle-joint will release electromagnetic radiation energy, which will be captured by the receiver in the MRI equipment. The energy will be converted into signal information in the receiver, and then converted into image information through computer encoding, calculation, and reconstruction processing. During MRI image extraction and DFIS data collection, the joint coils worn on the ankles of basketball players track and excite changes in the ankle-joint in real time, marking images of the ankle-joint at different times. At the same time, the DFIS also marks ankle-joint data at different times during data collection, and registers the image information and data at the same time using SIFT feature detection algorithm. The SIFT algorithm detects key-points by filtering MRI images in scale space, calculates the direction of each key-point, and finally generates feature descriptors. The data collected in the DFIS system is matched through the feature descriptors of the images, that is, image registration. When processing the images obtained by MRI technology, MRI image processing software can be used, which is a tool for MRI image processing and analysis. Various images of basketball players' ankle-joints are collected using MRI technology and registered with various data in the DFIS. Based on the registered data and images, 3D modeling of the ankle-joint bone structure is performed and bio-mechanical analysis of basketball players' ankles is conducted using this modeling. The specific flowchart of this process is shown in **Figure 5**.

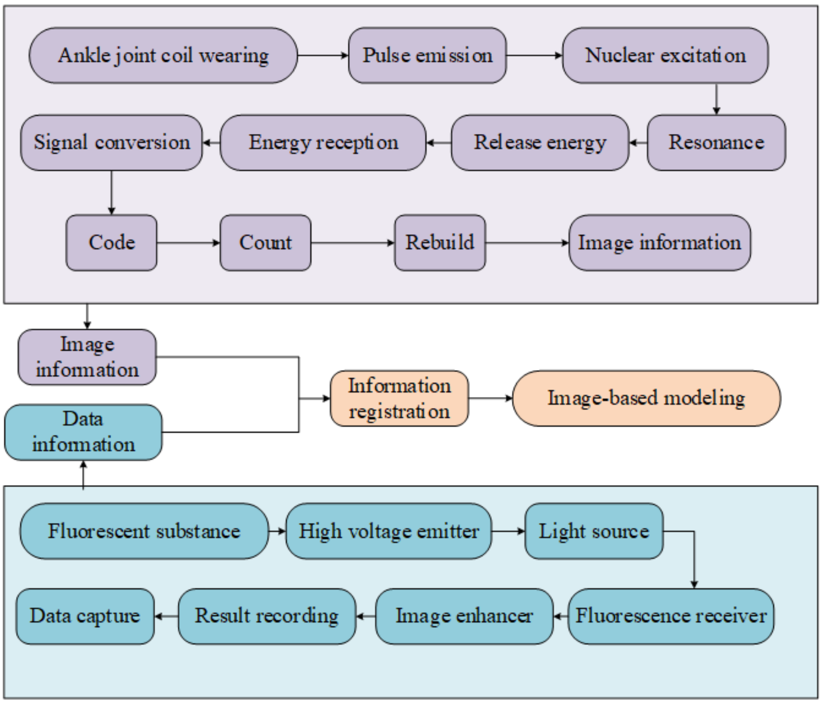

Figure 5. DFIS-MRI image modeling process.

By following the workflow in **Figure 5**, a three-dimensional model of the skeletal structure of the ankle-joint of a basketball player is established. When conducting bio-mechanical analysis, it is necessary to calculate the parameters of human biomechanics to ensure the accuracy of the analysis. The human ankle-joint, also known as the calf-joint, requires calculation of various bio-mechanical parameters of the calf during bio-mechanical analysis. The calculation method for the length and volume parameters of the calf is shown in Equation (7).

$$\begin{cases} L = 0.247H \\ V = 0.4083V_T \end{cases} \tag{7}$$

In Equation (7), L is the bio-mechanical parameter of calf length, V is the bio-mechanical parameter of calf volume, H is human height, and V_T is human volume. The calculation method for calf center of gravity and weight parameters is shown in Equation (8).

$$\begin{cases} Q = 0.433L \\ W = 0.042W_T \end{cases} \tag{8}$$

In Equation (8), Q represents the bio-mechanical parameter of the calf center of gravity, W represents the bio-mechanical parameter of calf weight, and W_T represents human body weight. The calculation formula for the calf rotation radius parameter is shown in Equation (9).

$$R = 0.528L \tag{9}$$

In Equation (9), R is the bio-mechanical parameter of the calf rotation radius. After calculating the bio-mechanical parameters of calf movement, the length and strain of ankle-joint ligaments need to be calculated based on the system's results to analyze the bio-mechanical situation of ankle-joint movement. The calculation for ligament length is shown in Equation (10).

$$L_a = \sqrt{(Mx - Nx)^2 + (My - Ny)^2 + (Mz - Nz)^2} \tag{10}$$

In Equation (10), (Mx, My, Mz) represents the coordinates of the center of gravity of the bone, and (Nx, Ny, Nz) represents the coordinates of the endpoints of the bone ligaments. The calculation method for ligament strain is shown in Equation (11).

$$\varepsilon = (L_{a0} - L_{a1})/L_{a0} \tag{11}$$

In Equation (11), L_{a0} represents the initial length and L_{a1} represents the length after deformation.

3. Results

3.1. Performance testing of DFIS-MRI method

In order to analyze the performance of DFIS-MRI method in data collection and imaging of ankle-joint, a comparative experiment was conducted between DFIS-MRI method and Mocap motion capture method, X-ray imaging method, and ultrasonic imaging (UI) equipment. The parameter requirements for various equipment during the experiment are shown in **Table 1**.

Table 1. Parameter setting of the experimental equipment.

Number	Parameter	Set up	Number	Parameter	Set up
1	Continuous exposure mode	1000 Hz	5	Sensor frequency	60–1000 fps
2	Shooting volume	40 × 40 × 40 cm^3	6	Area of the X-Ray collection area	> 43 × 43
3	Image resolution	1024 × 1024	7	X-Ray imaging pixels	> 9 million pixels
4	3 D positioning accuracy	< ± 0.1 mm	8	High speed pulse frequency	120 Hz

During the experiment, 100 basketball players from a certain hospital who require ankle-joint examination were randomly selected as experimental samples. The imaging effect of their ankle bone structure was analyzed to determine the effectiveness of the DFIS-MRI method. Firstly, the completeness of data collection was compared among the four methods, and the results are shown in **Figure 6**.

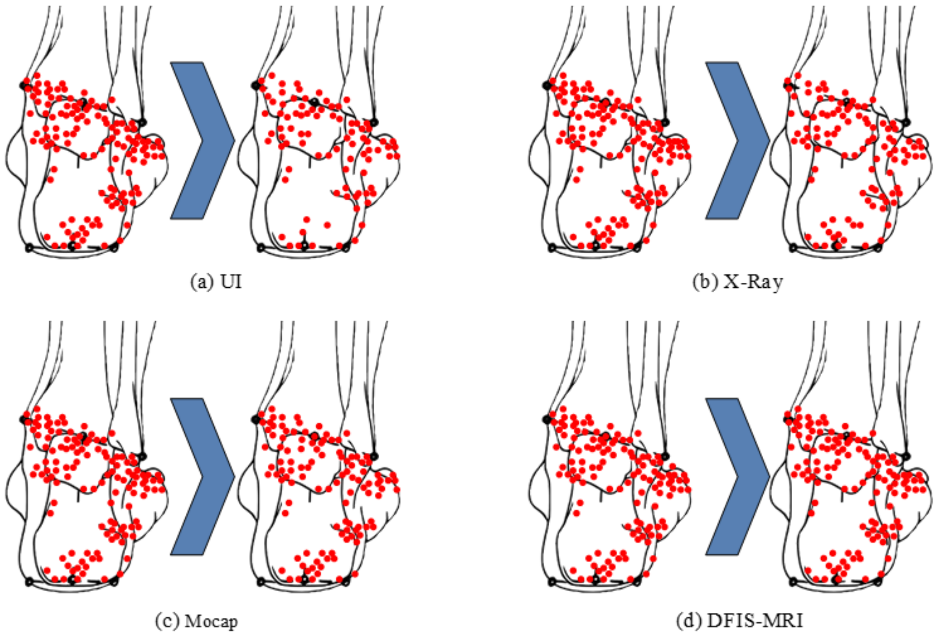

Figure 6. Comparison of data collection completeness across different methods. **(a)** UI; **(b)** X-Ray; **(c)** Mocap; **(d)** DFIS-MRI.

As shown in **Figure 6a**, the UI method had weak data collection integrity in the ankle-joint, and many data were missed. As shown in **Figure 6b**,**c**, the X-ray and Mocap imaging methods significantly improved the completeness of collecting ankle-joint image feature data. From **Figure 6d**, the DGIS-MRI method proposed in the study could collect all data of the ankle-joint completely, and the data collection effect was the best. Comparing the imaging effects of the four methods on ankle bone structure images, the results are shown in **Figure 7**.

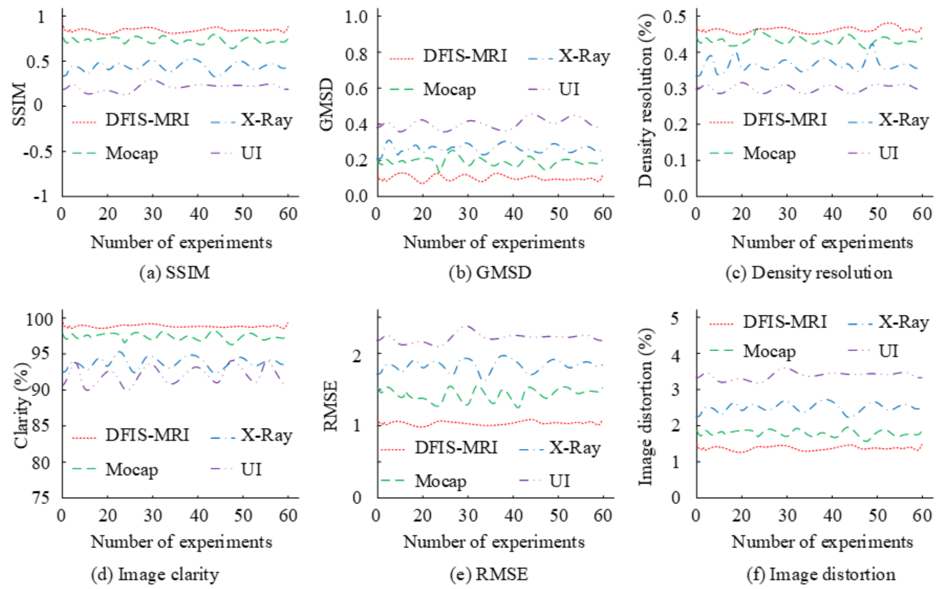

Figure 7. Imaging effect comparison. **(a)** SSIM; **(b)** GMSD; **(c)** Density resolution; **(d)** Image clarity; **(e)** RMSE; **(f)** Image distortion.

The SSIM value of an image represents the structural similarity index of the imaged image, the range of SSIM values is −1 to 1. The closer the SSIM value is to 1, the more similar the image obtained through system imaging is to the actual image. This indicator can better determine the imaging accuracy of the four imaging methods. According to **Figure 7a**, the SSIM value of the DFIS-MRI method was the highest, at 0.87, while the SSIM values of the X-Ray, Mocap, and UI methods were 0.86, 0.65, and 0.49, respectively, all lower than the DFIS-MRI method. The GMSD value is the gradient magnitude similarity deviation of the image, it is an indicator used to evaluate image quality, with a value range of 0 to 1. This indicator measures image quality by measuring the difference in gradient amplitude between the imaged image and the distorted image. The closer the value is to 1, the worse the image quality. From **Figure 7b**, the GMSD value of DFIS-MRI was significantly lower than other methods, with a GMSD value of 0.12. Image density resolution, also known as the contrast resolution of an image, refers to the ability to display the minimum density difference that can be seen in the image. The larger the value, the less noise and the larger the display in the image. According to **Figure 7c**, the density resolutions of DFIS-MRI method, X-Ray, Mocap, and UI method were 0.48%, 0.43%, 0.39%, and 0.32%, respectively. According to **Figure 7d–f**, the DFIS-MRI method had the highest image clarity of 98.7%, the lowest root mean square error of pixel differences in the image was only 0.96%, and the lowest distortion of the imaged image was only 1.43%. Finally, the imaging accuracy and artifact rate of the four methods were compared, and the results are shown in **Figure 8**.

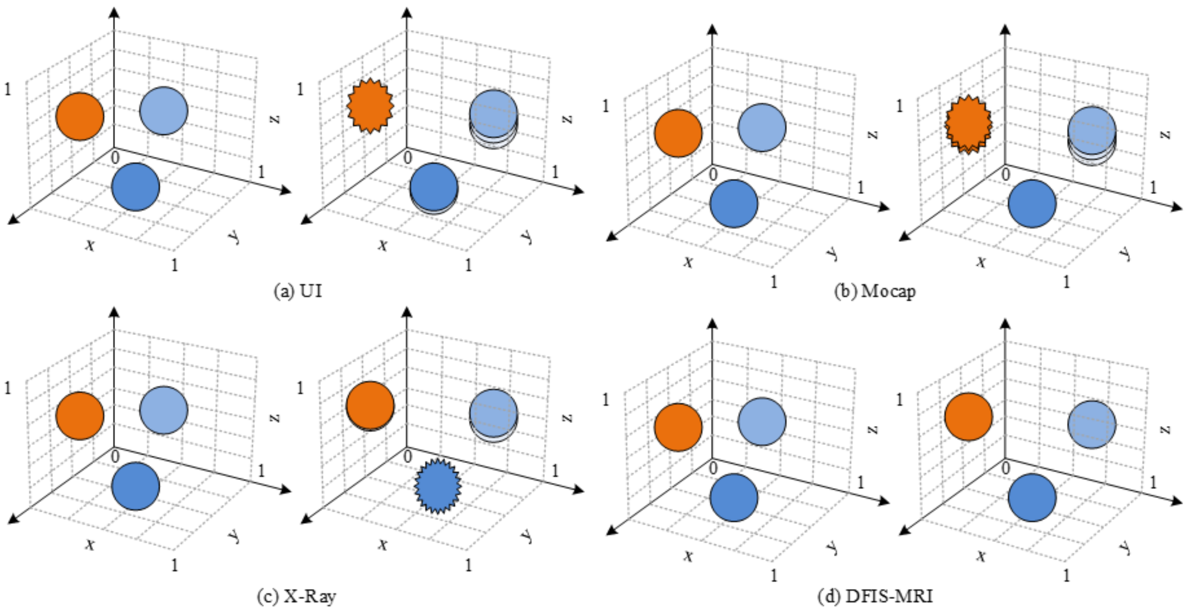

Figure 8. for imaging artifact rate comparison. **(a)** UI; **(b)** Mocap; **(c)** X-Ray; **(d)** DFIS-MRI.

Imaging artifacts refer to the overlapping, missing, or distorted images generated during the imaging process. From **Figure 8**, among the four imaging methods, only the DFIS-MRI method had the best imaging effect, which was consistent with the actual situation, while the images obtained by other medical imaging methods showed varying degrees of ghosting, overlapping, image deformation, and missing phenomena. From the above experimental results, the DFIS-MRI method could accurately present the skeletal structure in human joints, which was beneficial for subsequent analysis of skeletal structure and human biomechanics, and improved the accuracy of analysis.

3.2. Bio-mechanical analysis of ankle movements of basketball players based on DFIS-MRI technology

After testing the performance of the DFIS-MRI method proposed in the study, this method was then used to analyze the biomechanics of basketball players' movements and sports biomechanics. The study selected 50 basketball players to analyze their biomechanics under different shoe upper heights, in order to obtain the ankle dynamics characteristics of basketball players. The study first compared the maximum strain rates and strain values of various ligaments in the ankle of basketball players during lateral cutting movements. The analysis of 50 basketball players was averaged, and the results are shown in **Figure 9**.

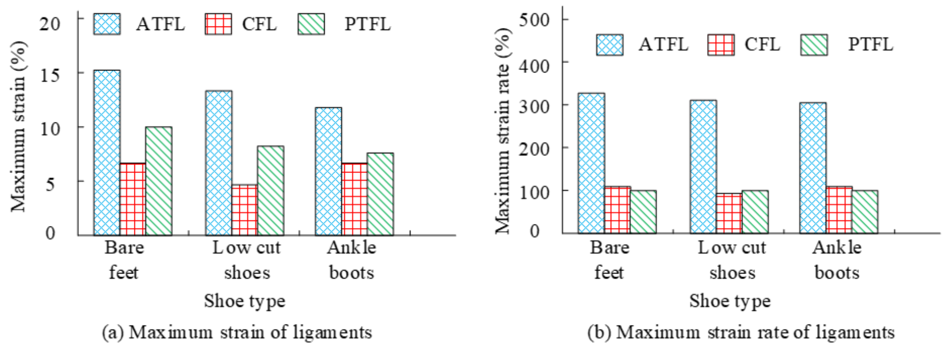

Figure 9. Maximum strain and strain rate of the ligament. **(a)** Maximum strain of ligaments;**(b)** Maximum strain rate of ligaments.

In **Figure 9**, CFL represents the calcaneofibular ligament of the human ankle, ATFL represents the anterior talofibular ligament of the human ankle, and PTFL represents the posterior talofibular ligament. According to **Figure 9a**, it can be seen that when a basketball player completed a lateral cut, the maximum strain of ATFL at the ankle was higher than the maximum strain values of CFL and PTFL. The maximum strains of ATFL, CFL, and PTFL wearing high top shoes were 13.5%, 5.6%, and 6.8%, respectively. The maximum strain of ATFL and PTFL was decreasing compared to barefoot and low-cut states, but the maximum strain of CFL was increasing. As shown in **Figure 9b**, wearing high top shoes could significantly reduce the maximum strain rate of the ATFL, reducing it to 296%. However, the reduction in maximum strain rate of the CFL and PTFL by high top shoes was not significant, and the effect was not significant. Comparing the on-stage speed and ankle-joint axial reaction force of basketball players during lateral cutting, the results are shown in **Figure 10**.

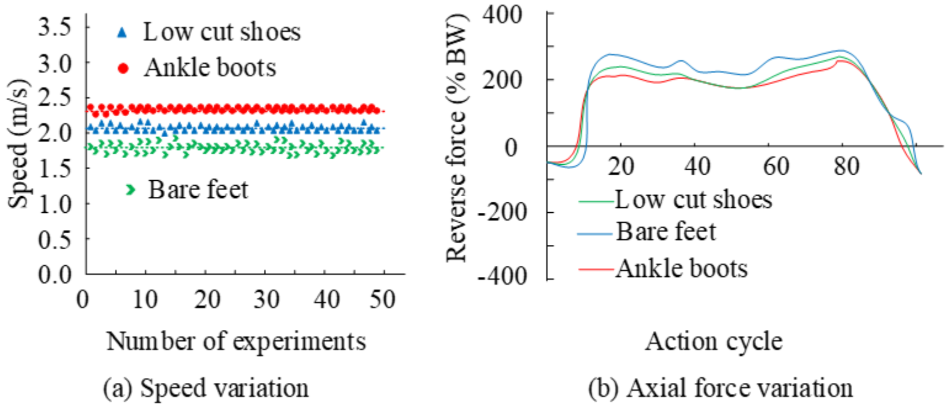

Figure 10. Stage velocity and ankle axial reaction force. **(a)** Speed variation; **(b)** Axial force variation.

The on-stage speed in sports biomechanics refers to the ability of athletes to convert horizontal velocity into vertical velocity during movements, which can reflect their athletic ability and efficiency in different situations. From **Figure 10a**, it can be seen that the on-stage speed of high top shoes was significantly higher than that of low top shoes and bare feet. In the cases of high top shoes, low top shoes, and bare feet, the average on-stage speed of basketball players was 2.23 m/s, 2.02 m/s, and 1.87 m/s, respectively. As shown in **Figure 10b**, when basketball players performed lateral cutting movements, the axial reaction force first increased, then stabilized, and finally decreased with the change of movement. Moreover, high top shoes could reduce the axial reaction force of athletes. Finally, a comparison was made between the reaction forces of the ankle inside and outside, front and back, and vertical ground during different stages of lateral cutting movements performed by basketball players under different shoe upper heights, in order to analyze the biomechanics of basketball players' movements. The results are shown in **Table 2**.

Table 2. Changes in ankle reaction forces at different stages.

Counterforce	Action Cycle (%)	Bare Feet	Low Cut Shoes	Ankle Boots
Internal and External Surface Reaction Force (% BW)	20	20 ± 0.45	23 ± 0.41	24 ± 0.42
	40	43 ± 0.34	48 ± 0.43	47 ± 0.46
	60	56 ± 0.46	60 ± 0.44	61 ± 0.41
	80	50 ± 0.53	57 ± 0.43	56 ± 0.45
Front and Rear Ground Reaction Force (% BW)	20	52 ± 0.47	56 ± 0.39	57 ± 0.39
	40	47 ± 0.49	53 ± 0.47	54 ± 0.42
	60	42 ± 0.78	46 ± 0.45	48 ± 0.37
	80	37 ± 0.45	42 ± 0.35	40 ± 0.40
Vertical Ground Reaction Force (% BW)	20	121 ± 0.41	123 ± 0.43	122 ± 0.43
	40	150 ± 0.56	153 ± 0.48	152 ± 0.37
	60	143 ± 0.51	145 ± 0.41	142 ± 0.47
	80	138 ± 0.46	137 ± 0.45	138 ± 0.45

According to **Table 2**, when basketball players completed lateral cutting movements, as the movement cycle increased, the ground reaction forces in the inner and outer directions of the ankle-joint, the ground reaction forces in the front and rear directions, and the vertical reaction force all increased first and then decreased. The horizontal reaction force of the ankle-joint in the state of high top and low top shoes for athletes was roughly the same, and both were greater than the reaction force under barefoot conditions. In the three cases, the difference in vertical ground reaction force was relatively low and there was no significant difference.

4. Discussion and conclusion

This study aimed to address the issues of image blurring and data loss in current bio-mechanical analysis of ankle movements in basketball players. The DFIS was integrated with MRI technology, and an image model for bio-mechanical analysis of movements was constructed based on the fused technology. To verify the superiority of the DFIS-MRI method, a comparative experiment was conducted between the DFIS-MRI method and the widely used X-ray method, Mocap method, and UI method. The experiment outcomes showed that the DFIS-MRI method had the highest completeness of bone data collection, while the UI method had the lowest completeness of data collection. Moreover, the DFIS-MRI method did not produce artifacts when imaging bone structures, avoiding errors in subsequent bio-mechanical analysis. This result is similar to that of the He et al. [18]. The reason for this result may be that MRI technology can accurately extract image information of bone structures through MRI, improve image accuracy, and reduce the occurrence of artifacts. The SSIM value of the DFIS-MRI system was 0.87, the GMSD value was 0.12, and the image clarity was 98.7%, all of which were superior to other imaging methods. This result is roughly consistent with Ma et al.'s [19] results, and the reason for this change may be that the combination of DFIS and MRI technology can register bone map information and bone data, improving image clarity and imaging effect. Using the above method again, the biomechanics of basketball players when formulating movements at different shoe heights were analyzed. The results showed that in the high top shoe state, the maximum strain of ATFL in the ankle was 13.5%, much lower than that in the low top state and bare foot state, and its maximum strain rate was significantly reduced. However, although the maximum strain of CFL and PTFL in the ankle decreased in the high top state, the magnitude of their maximum strain rate changes was not significant and almost unchanged, which coincides with Lam et al.'s [20] results. From the above results, it can be concluded that athletes wearing high top shoes can reduce the maximum strain value and maximum strain rate of the anterior talofibular ligament in the ankle-joint during exercise, thereby providing protection for the athlete's ankle. Through analysis of the biomechanics of ankle-joint movement, it can be found that in the high top shoe state, the athlete's ascent speed reached 2.23 m/s, higher than the 2.02 m/s of low top shoes and the 1.87 m/s of bare feet. However, the axial reaction force of the ankle-joint was significantly reduced in the high top shoe state, which is similar to the experimental results of Rowe et al.'s [21] team. From this result, it can be concluded that high top shoes can reduce the axial reaction force of the ankle-joint, thereby reducing the risk of ankle-joint injury. Aiello et al. [22] analyzed the biomechanics of football players' ankles and found that high top shoes can also provide better protection for the ankles during football related sports. Aiello et al. investigated 56,740 football injury incidents and found that the ankle injury rate of low top shoe athletes was much higher than that of high top shoe athletes, which is consistent with the results of this study. However, Aiello et al.'s study also found that although high top shoes can help football players reduce ankle injuries, they can affect their movement speed and flexibility. So, Aiello et al. suggested that if a player is heavy and strong, they need to engage in frequent internal confrontations and are suitable for wearing high top shoes; If players need to move quickly or indirectly, low top shoes are more suitable.

From the above results, it can be seen that the DFIS-MRI method proposed in the study can improve the accuracy and quality of medical image imaging. Through this method, it was found that when basketball players perform side cutting movements, due to the higher upper of high top shoes, high top shoes can reduce the maximum strain in ankle biomechanics during lateral cutting movements of basketball players, increase their on-stage speed, reduce axial reaction forces, and thus reduce ankle injuries. It can effectively support and protect the ankle, reducing the risk of sprains or sprains caused by jumping, turning, and other movements during athletes' exercise. The design of high top shoes can provide better lateral stability for athletes, helping them better complete complex sports movements. In addition, high top shoes are often equipped with excellent cushioning systems, which can effectively reduce the intense vibration of the lower limbs of basketball players during side cutting movements and lower the risk of lower limb injuries during exercise. So, basketball players can protect themselves by wearing high top shoes when performing side cuts. However, due to venue limitations, this study only analyzed the ankle biomechanics of basketball players' lateral cutting movements. Basketball also includes other common movements such as shooting, passing, defense, and sliding. Conducting bio-mechanical research on other common basketball movements can help teachers focus on explaining bio-mechanical knowledge to students in physical education courses. This allows students to find suitable exercise techniques and training methods, and helps basketball players better protect their own safety and reduce physical injuries. So, in the future, bio-mechanical analysis of basketball players' complete movements should also be conducted.

Ethical approval: Not applicable.

Conflict of interest: The author declares no conflict of interest.

References

1. Morrison M, Martin D T, Talpey S. A systematic review on fitness testing in adult male basketball players: Tests adopted, characteristics reported and recommendations for practice. Sports Medicine, 2022, 52(7): 1491-1532.
2. Haïdara Y, Okilanda A, Dewintha R, Suryadi, D. Analysis of students' basic basketball skills: A comparative study of male and female students. Tanjungpura Journal of Coaching Research, 2023, 1(1): 1-5.
3. Lin T, Chen Z, Yang Y, Chiappalupi D, Beyer J, Pfister H. The quest for omnioculars: Embedded visualization for augmenting basketball game viewing experiences. IEEE transactions on visualization and computer graphics, 2022, 29(1): 962-971.
4. Megalaa T, Hiller C E, Ferreira G E, Beckenkamp P R, Pappas E. The effect of ankle supports on lower limb biomechanics during functional tasks: A systematic review with meta-analysis. Journal of Science and Medicine in Sport, 2022, 25(7): 615-630.

5. Hughes G T G, Camomilla V, Vanwanseele B, Harrison A J, Fong D T, Bradshaw E J. Novel technology in sports biomechanics: Some words of caution. Sports Biomechanics, 2024, 23(4): 393-401.
6. Blanco Ortega A, Isidro Godoy J, Szwedowicz Wasik D S, et al. Biomechanics of the upper limbs: A review in the sports combat ambit highlighting wearable sensors. Sensors, 2022, 22(13): 4905-4912.
7. Yu P, Mei Q, Xiang L, Fernandez J, Gu Y. Differences in the locomotion biomechanics and dynamic postural control between individuals with chronic ankle instability and copers: a systematic review. Sports Biomechanics, 2022, 21(4): 531-549.
8. Koldenhoven R M, Hart J, Abel M F, et al. Running gait biomechanics in females with chronic ankle instability and ankle sprain copers. Sports biomechanics, 2022, 21(4): 447-459.
9. Wang L, Ye J, Zhang X. Ankle biomechanics of the three-step layup in a basketball player with chronic ankle instability. Scientific Reports, 2023, 13(1): 18667-18678.
10. Domínguez-Navarro F, Benitez-Martínez J C, Ricart-Luna B. Impact of hip abductor and adductor strength on dynamic balance and ankle biomechanics in young elite female basketball players. Scientific Reports, 2022, 12(1): 3491.
11. Dietze M M A, Kunnen B, Brontsema F, Ramaekers P, Beijst C, Afifah M. A compact and mobile hybrid C-arm scanner for simultaneous nuclear and fluoroscopic image guidance. European Radiology, 2022, 32(1): 517-523.
12. Wu C, Wang Y, Wang C, Chen J, Xu J, Yu W, Xie G. Glenoid track width is smaller under dynamic conditions: an in vivo dual-fluoroscopy imaging study. The American Journal of Sports Medicine, 2022, 50(14): 3881-3888.
13. Hugosson J, Godtman R A, Wallstrom J, et al. Results after Four Years of Screening for Prostate Cancer with PSA and MRI. New England Journal of Medicine, 2024, 391(12): 1083-1095.
14. Arnold T C, Freeman C W, Litt B, Stein J M. Low-field MRI: clinical promise and challenges. Journal of Magnetic Resonance Imaging, 2023, 57(1): 25-44.
15. Bertozzi F, Fischer P D, Hutchison K A, Zago M, Sforza C, Monfort S M. Associations between cognitive function and ACL injury-related biomechanics: a systematic review. Sports health, 2023, 15(6): 855-866.
16. Ariztia J, Solmont K, Moïse N P, Specklin S, Heck M P, Lamande-Langle S, Kuhnast B. PET/fluorescence imaging: An overview of the chemical strategies to build dual imaging tools. Bioconjugate Chemistry, 2022, 33(1): 24-52.
17. Charidimou A, Boulouis G, Frosch M P, Baron J C, Pasi M, Albucher J F. The Boston criteria version 2.0 for cerebral amyloid angiopathy: a multicentre, retrospective, MRI–neuropathology diagnostic accuracy study. The Lancet Neurology, 2022, 21(8): 714-725.
18. He S, Bhatt R, Brown C, Brown E A, Buhr D L, Chantranuvatana K, Beechem J M. High-plex imaging of RNA and proteins at subcellular resolution in fixed tissue by spatial molecular imaging. Nature Biotechnology, 2022, 40(12): 1794-1806.
19. Ma W, Su Y, Zhang Q, Deng C, Pasquali L. Thermally activated delayed fluorescence (TADF) organic molecules for efficient X-ray scintillation and imaging. Nature materials, 2022, 21(2): 210-216.
20. Lam W K, Jia S W, Baker J S, Ugbolue U C. Effect of consecutive jumping trials on metatarsophalangeal, ankle, and knee biomechanics during take-off and landing. European Journal of Sport Science, 2021, 21(1): 53-60.
21. Rowe P L, Bryant A L, Egerton T, Paterson K L. External Ankle Support and Ankle Biomechanics in Chronic Ankle Instability: Systematic Review and Meta-Analysis. Journal of Athletic Training, 2023, 58(7-8): 635-647.
22. Aiello F, Impellizzeri F M, Brown S J. Injury-inciting activities in male and female football players: a systematic review. Sports medicine, 2023, 53(1): 151-176.